Voltage controlled modification of flux closure domains in planar magnetic structures for microwave applications

Cite as: Appl. Phys. Lett. **105**, 062405 (2014); https://doi.org/10.1063/1.4892942
Submitted: 30 May 2014 • Accepted: 29 July 2014 • Published Online: 13 August 2014

D. E. Parkes, R. Beardsley, S. Bowe, et al.

Voltage controlled modification of flux closure domains in planar magnetic structures for microwave applications

D. E. Parkes,[1] R. Beardsley,[1] S. Bowe,[1,2] I. Isakov,[3] P. A. Warburton,[3] K. W. Edmonds,[1] R. P. Campion,[1] B. L. Gallagher,[1] A. W. Rushforth,[1,a)] and S. A. Cavill[4,2,a)]
[1]*School of Physics and Astronomy, The University of Nottingham, Nottingham NG7 2RD, United Kingdom*
[2]*Diamond Light Source, Chilton, Didcot, Oxfordshire OX11 0DE, United Kingdom*
[3]*London Centre of Nanotechnology, University College London, London WC1H 0AH, United Kingdom*
[4]*Department of Physics, University of York, Heslington, York YO10 5DD, United Kingdom*

(Received 30 May 2014; accepted 29 July 2014; published online 13 August 2014)

Voltage controlled modification of the magnetocrystalline anisotropy in a hybrid piezoelectric/ferromagnet device has been studied using Photoemission Electron Microscopy with X-ray magnetic circular dichroism as the contrast mechanism. The experimental results demonstrate that the large magnetostriction of the epitaxial $Fe_{81}Ga_{19}$ layer enables significant modification of the domain pattern in laterally confined disc structures. In addition, micromagnetic simulations demonstrate that the strain induced modification of the magnetic anisotropy allows for voltage tuneability of the natural resonance of both the confined spin wave modes and the vortex motion. These results demonstrate the possibility for using voltage induced strain in low-power voltage tuneable magnetic microwave oscillators.
[http://dx.doi.org/10.1063/1.4892942]

Lateral confinement in planar magnetic materials leads to the formation of well defined magnetic domain patterns. The Landau flux closure and vortex domain configurations are the most obvious examples, and interest in these has been renewed recently due to the possibility of using a vortex structure in a four state memory device,[1] where the chirality and direction of the vortex encode the four possible states. In addition domain configurations with vortex states are currently heavily investigated for magnetic resonator applications.[2] The interest in microwave technologies relies on the fact that under the correct conditions, a spin polarized current transfers angular momentum to the magnetic structure, the Spin Transfer Torque (STT), giving rise to sustained oscillations at microwave frequencies. STT has found applications in a wide range of research areas including non-volatile information storage, such as STT-magnetic random access memory (STT-MRAM)[3] and domain-wall race-track memory,[4] as well as in magnetic microwave oscillators commonly known as spin-torque oscillators (STOs) or spin torque vortex oscillators (STVOs), if a vortex state is present.[2,5] These structures are of great commercial interest due to the fact that they are highly tuneable and very large scale integration (VLSI) compatible. However, a number of challenges need to be addressed before widespread applications of STVOs are possible including increasing the output power, removing the need for large applied magnetic fields and reducing device-to-device variations. Schemes to increase the output power of STVOs have been a topic of intense research with phase locking an array of oscillators being the most elegant.[6] An important aspect of phase locking is the ability to control the phase and frequency of the oscillator with respect to a reference oscillator or other oscillators in an array. Fortunately, STVO frequencies can be varied with both applied magnetic field and current. Tuning the oscillator frequency using an applied magnetic field has obvious difficulties related to addressing individual elements in an array, whilst tuning by changing the bias current leads to issues with energy dissipation. A possible solution to this problem would be to use a material in the STVO, which can be tuned over a large frequency range by the application of an electric field rather than a current. Modification of magnetization and magnetocrystalline anisotropy (MCA) by electric fields is therefore highly desirable for data storage, spintronic, and microwave applications alike. Electric field manipulation of magnetization has been reported previously for ferromagnetic semiconductors,[7] single phase multiferroics,[8] interface magneto-electric effects,[9] and via strain induced in ferromagnet/piezoelectric hybrid devices.[10,11] In this paper, we demonstrate that the application of uniaxial strain to magnetostrictive microstructures allows for the reversible modification of the flux closure domain pattern. Moreover, we show that the fundamental precessional frequency of the confined spin wave modes and of the vortex core is strongly modified by the strain over the experimentally accessible range.

The experimental system studied consisted of a 14 nm $Fe_{81}Ga_{19}$ epitaxial thin film grown by molecular beam epitaxy on a *n*-doped GaAs buffered GaAs(001) substrate. A 1.5 nm amorphous GaAs capping layer was grown to protect the metallic layer from oxidation. Previous investigations of films grown under similar conditions[10] showed that the $Fe_{81}Ga_{19}$ grows as a single crystal on GaAs(001). Superconducting Quantum Interference Device (SQUID) magnetometry reveals that the in-plane magnetic anisotropy consists of a superposition of a cubic term ($K_c = 18.9\,kJm^{-3}$) favouring the [100]/[010] directions and a uniaxial term ($K_u = 12.4\,kJm^{-3}$) along the [110] direction.

a)Authors to whom correspondence should be addressed. Electronic addresses: Stuart.Cavill@york.ac.uk and Andrew.Rushforth@nottingham.ac.uk.

The uniaxial anisotropy directed along the [110] direction is induced by the GaAs substrate as also observed in thin Fe films grown epitaxially on GaAs (001).[12] The 2.2 μm diameter disc structures were fabricated by electron beam lithography and Ar ion milling before the substrate was thinned to 150 μm and bonded to a piezoelectric lead zirconante titanate (PZT) transducer, following the procedure in Ref. 10. Magnetic domains were imaged using the X-ray Photoemission electron microscope (PEEM) on beamline I06 at the Diamond Light Source synchrotron. Illuminating the sample at oblique incidence and making use of X-ray magnetic circular dichroism (XMCD) at the Fe L_3 edge as the contrast mechanism allowed sensitivity to in-plane moments with a spatial resolution of approximately 50 nm.

Figure 1(b) shows the magnetic domain pattern for a 2.2 μm diameter $Fe_{81}Ga_{19}$ disc with a voltage, $V_p = 0$ V, applied to the PZT transducer. The disc structure forms a Landau flux closure domain pattern similar to that normally found in square planar elements. The magnetic domains form this pattern instead of the usual curling vortex structure, commonly found in disc elements, due to the strong cubic MCA in the material which forces the magnetic moments to lie along the cubic [100] and [010] directions. Indeed, for a structure of this size, the cubic MCA term for the $Fe_{81}Ga_{19}$ film dominates over the in-plane or "longitudinal" shape anisotropy. Of particular interest is that the domains whose moments point along the [010] direction, shown as grey in Fig. 1(b), are larger in area than the domains with moments pointing perpendicular to this axis. Previous work on these hybrid piezoelectric/magnetostrictive devices[13] has demonstrated that a finite strain occurs, even for zero voltage on the transducer. This effect is due to the anisotropic thermal expansion of the transducer during the bonding process, which induces a uniaxial tensile strain of order 10^{-4}. We confirm this by performing micromagnetic simulations using the Object Oriented Micromagnetic Framework (OOMMF)[14] with a mesh size of 2 nm × 2 nm × 10 nm and both cubic ($K_c = 18.9\,kJm^{-3}$) and uniaxial ($K_u = 12.4\,kJm^{-3}$) magnetocrystalline anisotropy terms. The strain induced anisotropy is included as an extra uniaxial term (K_s) along the [010] direction. In order to obtain good agreement between the experimental data of Fig. 1(b) and the simulation, we have to include a positive non-zero strain induced anisotropy term ($K_s = 3.5\,kJm^{-3}$) as shown in Fig. 1(f). By applying −40 V to the piezoelectric transducer, the strain induced during fabrication is approximately compensated, resulting in domains of similar size as shown in Fig. 1(a). Again good agreement is found with the micromagnetic simulations by setting $K_s = 0$. The domain configuration for $V_p = +60$ V and +80 V are shown in Figs. 1(c) and 1(d), respectively. At these voltages, a large uniaxial tensile strain is induced along the [010] direction in addition to that from the fabrication process and dominates the magnetocrystalline components favouring domains which align along the [010] direction. The domains which initially align along the [100] direction are reduced in area to such an extent in the central region of the disc that, to within the resolution of the PEEM, they resemble a domain wall. Setting $K_s = 8.4\,kJm^{-3}$ and $10\,kJm^{-3}$ in the micromagnetic simulation gives excellent agreement to the experimental data, Figs. 1(g) and 1(h). Using results obtained from previous studies of $Fe_{81}Ga_{19}$ on PZT transducers,[13] the application of +80 V to the piezoelectric transducer applies approximately 6×10^{-4} strain to the $Fe_{81}Ga_{19}$ film. The magnetoelastic energy induced by the applied strain is given by

$$E_{ME} = B_1(\epsilon_{xx} - \epsilon_{yy})\sin^2\phi, \quad (1)$$

where $B_1 = 3/2\lambda_{100}(C_{12} - C_{11})$, λ_{100} is the magnetostriction constant, C_{12} and C_{11} are the elastic constants, ϕ is the angle between the applied strain and the [010] axis, and ϵ_{xx}, ϵ_{yy} are the relevant components of the strain tensor. In order to produce large changes in the magnetic system for a given strain, it is important to maximise B_1—the magnetoelastic constant. For our $Fe_{81}Ga_{19}$ thin films, B_1 is approximately16 MJm^{-3}.[15] Therefore, an applied strain of 6×10^{-4} results in a magnetoelastic energy of approximately $10\,kJm^{-3}$, which is the value used in the micromagnetic simulation.

We next demonstrate the potential for strain induced changes in the magnetic energy and domain pattern for applications in microwave oscillators. Using the domain configuration and micromagnetic parameters in Figs. 1(e) and 1(h), we simulate the dynamic response of the magnetization to a 70 ps field pulse as shown in Fig. 2. In order to obtain good statistics, we set the damping parameter, α, to a factor of 10 lower than the experimentally observed value. The component of the magnetization along the [100] axis, M_x, is shown as a function of time delay after the field pulse in Figs. 3 and 4 for strain states corresponding to −40 V and

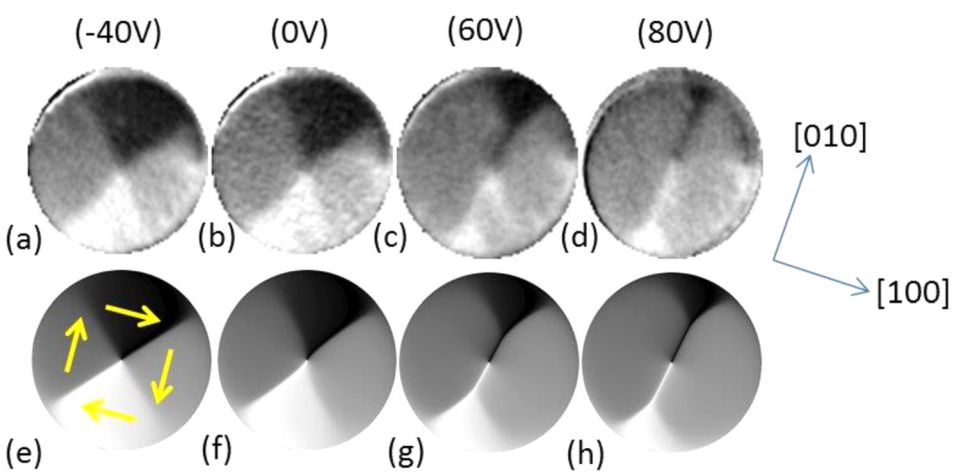

FIG. 1. Evolution of the magnetic domain pattern in a 2.2 μm circular FeGa/PZT structure for different voltages applied to the PZT transducer (top). Micromagnetic simulation of the 2.2 μm FeGa/PZT device (bottom) with K_s equal to (e) 0, (f) 3.5, (g) 8.4, and (h) $10\,kJm^{-3}$. The yellow arrows indicate the direction of magnetization in each domain.

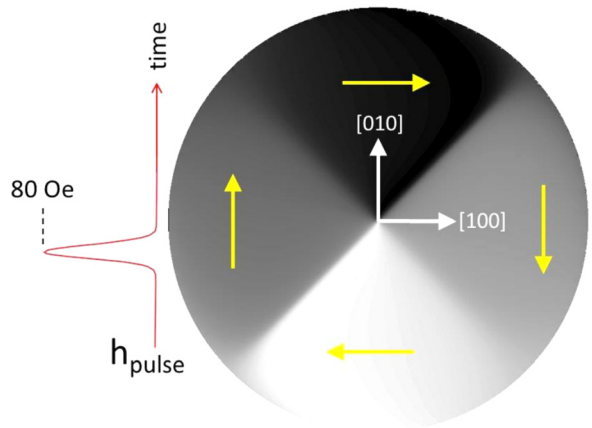

FIG. 2. Schematic diagram showing the direction of the field pulse with respect to the magnetization (yellow arrows) for $K_s = 0$. The field pulse is along the vertical [010] direction.

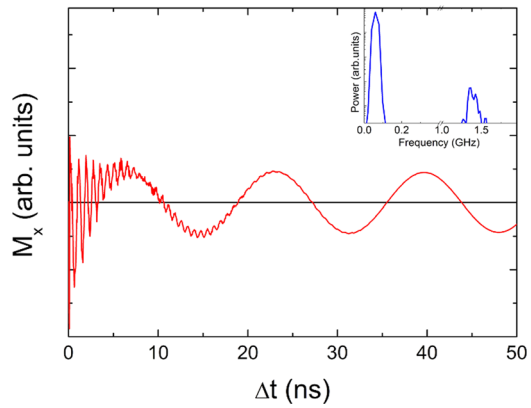

FIG. 3. The integrated x-component of the simulated magnetization, M_x, as a function of time after the perturbing field pulse for -40 V applied to the PZT transducer ($K_s = 0$). The inset shows the FFT of the data.

$+80$ V applied to the PZT transducer, respectively. As can be seen in Fig. 3, M_x shows the expected damped harmonic motion for a weakly perturbed magnetic system.

Two frequency components are clearly present: a fast oscillation with a period of approximately $\tau = 0.71$ ns and a slower oscillation with a period of approximately 16 ns. A fast Fourier transform (FFT) of the data, inset in Fig. 3, shows clear peaks at $f_1 = 60$ MHz and $f_2 = 1.4$ GHz, which correspond to the motion of the vortex core and the confined spin wave modes, respectively. The peak at high frequency is relatively broad due to the contribution of a number of confined spin wave modes quite close in frequency as expected for the Landau flux closure state. For a given excitation pulse, only certain modes are excited with the frequency spacing between adjacent modes dependent on the size of the structure. For relatively large dots, the observed peaks are expected to be composite ones. The effect on the dynamics of setting $K_s = 10\,\mathrm{kJm^{-3}}$, corresponding to $+80$ V applied to the PZT transducer, is shown in Fig. 4. Both the fast and slow oscillatory motions are still present but have now shifted in frequency to $f_1 = 25$ MHz and $f_2 = 1.2$ GHz for the vortex and spin wave modes. Thus, by using a voltage controlled strain we are able to tune the resonant frequency of both the spin wave mode and the vortex gyration by 14% and 58% over the experimentally accessible range of strain with respect to the zero strain state. In addition, the linewidth of the confined spinwave modes is considerably reduced. For this domain configuration and excitation pulse, fewer modes are excited compared to the unstrained state. Spectral linewidth is an important issue for practical implementations of STOs and here we demonstrate a way to modify the excited modes. Finally, we show how the voltage induced strain in this composite material changes not only the vortex gyration frequency but also its orbit. Fig. 5 shows the simulated orbital motion of the vortex core. When $K_s = 0\,\mathrm{kJm^{-3}}$, corresponding to -40 V applied to the PZT transducer, the vortex core sweeps out an approximately circular orbit with almost equal displacement in both x and y directions. The deviation from a perfect circular orbit is due to the intrinsic uniaxial anisotropy along the [110] direction. In comparison, for $K_s = 10\,\mathrm{kJm^{-3}}$, corresponding to $+80$ V applied to the PZT transducer, the vortex orbit becomes more elliptical, with the major axis of the ellipse close to the axis of tensile strain.

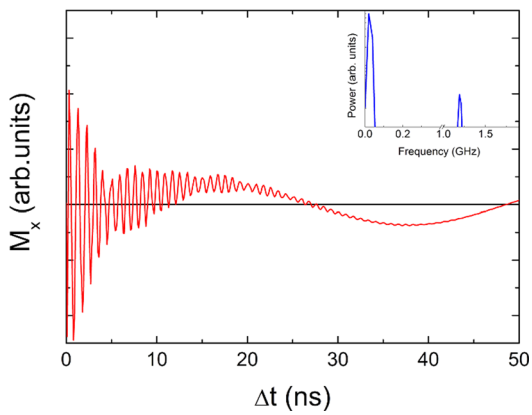

FIG. 4. The integrated x-component of the simulated magnetization, M_x, as a function of time after the perturbing field pulse for $+80$ V applied to the PZT transducer ($K_s = 10\,\mathrm{kJm^{-3}}$). The inset shows the FFT of the data.

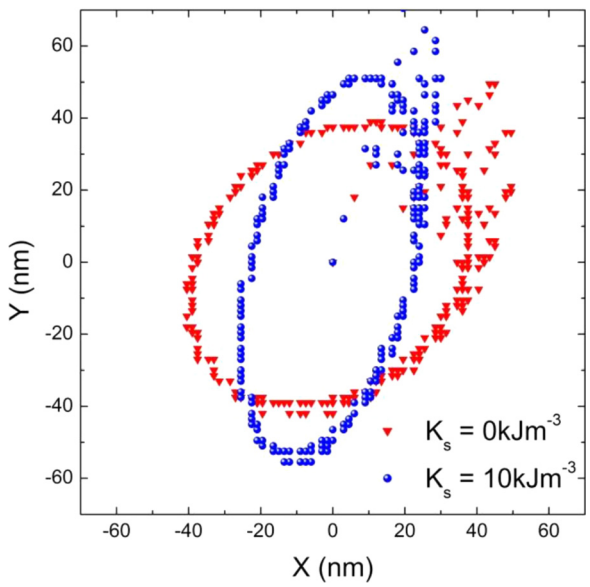

FIG. 5. Co-ordinates of the vortex core (simulated) after excitation with a 70 ps field pulse for $V_p = -40$ V (red triangles) and $+80$ V (blue circles). The field pulse is along the [010] y axis. The scatter in the data points in the positive x and y quadrant is due the effect of the field pulse and spin wave modes shortly after the field pulse.

In summary, we demonstrate that voltage induced strain in hybrid piezoelectric-magnetostrictive micro-structures significantly changes the magnetic domain configuration. Due to the strong restoring force of the shape and magnetocrystalline anisotropies, the voltage induced changes are reversible and volatile unlike previous work on macroscopic devices.[10] Using the micromagnetic simulation package OOMMF, the magnetization dynamics of the system have been studied at the two extreme strain conditions accessible in this particular device structure. By using a 80 Oe, 70 ps field pulse as the perturbation our simulations show that a voltage induced strain can significantly modify the spin wave mode and the vortex gyration frequencies and the spatial orbit of the vortex core gyration. By assembling similar magnetic structures directly onto piezoelectric substrates, such as $[Pb(Mg_{1/3}Nb_{2/3})O_3]_{(1-x)}$-$[PbTiO_3]_x$ (PMN-PT) and fabricating voltage electrodes with micrometre spacing it would be possible to achieve even larger strains for smaller applied voltages (of order <5 V). These results demonstrate the potential for hybrid multiferroics in voltage tuneable microwave oscillators.

The authors would like to acknowledge Diamond Light Source for the provision of beamtime under SI-8560, and EPSRC Grant EP/H003487/1.

[1]V. Uhlier, M. Urbanek, L. Hladik, J. Spousta, M.-Y. Im, P. Fischer, N. Eibagi, J. J. Kan, E. E. Fullerton, and T. Sikola, Nat. Nanotechnol. **8**, 341 (2013).
[2]V. S. Pribiag, I. N. Krivorotov, G. D. Fuchs, P. M. Braganca, O. Ozatay, J. C. Sankey, D. C. Ralph, and R. A. Burham, Nat. Phys. **3**, 498 (2007).
[3]H. Liu, D. Bedau, D. Backes, J. A. Katine, J. Langer, and A. D. Kent, Appl. Phys. Lett. **97**, 242510 (2010).
[4]S. S. P. Parkin, M. Hayashi, and L. Thomas, Science **320**, 190 (2008).
[5]S. I. Kiselev, J. C. Sankey, I. N. Krivorotov, N. C. Emley, R. J. Schoelkopf, R. A. Buhrman, and D. C. Ralph, Nature **425**, 380 (2003).
[6]F. B. Mancoff, N. D. Rizzo, B. N. Engel, and S. Tehrani, Nature **437**, 393 (2005).
[7]H. Ohno, D. Chiba, F. Matsukura, T. Omiya, E. Abe, T. Dietl, Y. Ohno, and K. Ohtani, Nature **408**, 944 (2000).
[8]W. Eerenstein, N. D. Mathur, and J. F. Scott, Nature **442**, 759 (2006).
[9]K. Ohta, T. Maruyama, T. Nozaki, M. Shiraishi, T. Shinjo, Y. Suzuki, S.-S. Ha, C.-Y. You, and W. Van Roy, Appl. Phys. Lett. **94**, 032501 (2009).
[10]D. E. Parkes, S. A. Cavill, A. T. Hindmarch, P. Wadley, F. McGee, C. R. Staddon, K. W. Edmonds, R. P. Campion, B. L. Gallagher, and A. W. Rushforth, Appl. Phys. Lett. **101**, 072402 (2012).
[11]M. Overby, A. Chernyshov, L. P. Rokhinson, X. Liu, and J. K. Furdyna, Appl. Phys. Lett. **92**, 192501 (2008).
[12]G. Wastlbauser and J. A. C. Bland, Adv. Phys. **54**, 137 (2005).
[13]S. A. Cavill, D. E. Parkes, J. Miguel, S. S. Dhesi, K. W. Edmonds, R. P. Campion, and A. W. Rushforth. Appl. Phys. Lett. **102**, 032405 (2013).
[14]M. J. Donahue and D. G. Porter, Interagency Report NISTIR 6376, National Institute of Standards and Technology, Gaithersburg, MD, September 1999.
[15]D. E. Parkes, L. R. Shelford, P. Wadley, V. Holy, M. Wang, A. T. Hindmarch, G. van der Laan, R. P. Campion, K. W. Edmonds, S. A. Cavill, and A. W. Rushforth, Sci. Rep. **3**, 2220 (2013).